JOURNAL OF MAGNETIC RESONANCE **130,** 341–345 (1998)
ARTICLE NO. MN971323

Improved Resolution from Double Constant-Time Evolution of 3D and 4D Triple-Resonance Experiments

Mark A. McCoy

The Wistar Institute, 36th and Spruce Streets, Philadelphia, Pennsylvania 19104; and Department of Chemistry, University of Pennsylvania, Philadelphia, Pennsylvania 19104

Received July 15, 1997; revised October 29, 1997

Triple-resonance NMR experiments are nearly essential for performing backbone assignments of proteins larger than ~15 kDa. Our work extends the double constant-time (2CT) evolution scheme to triple-resonance 3D and 4D experiments. The modifications needed to accomplish 2CT evolution in triple resonance experiments are straight forward, are completely general, and consequently, will yield increased resolution for all out-and-back experiments. We expect that the increased resolution of experiments presented here will be useful in the study of larger proteins (>30 kDa) and in the study of highly helical proteins where ^{1}HN, ^{15}N, and ^{13}C dimensions are poorly dispersed.

Key Words: **triple-resonance; constant-time; NMR.**

Triple-resonance heteronuclear correlation experiments are nearly essential for performing backbone assignments of proteins larger than ~15 kDa. The initial experiments (*1, 2*) have been extensively modified to include, for example, single-quantum evolution (*3*), constant-time (CT) evolution during polarization transfer periods (*3, 4*), sensitivity enhancement (*5*), water flip-back (*6*), and reduction of scalar relaxation (*3*). The work of Madsen and Sørensen (*7*) first demonstrated that both the forward and backward CT polarization transfer periods in ''out-and-back'' HNX experiments (X = C′, C_α, H_α) could be used to evolve ^{15}N coherence. In their scheme, which doubles the maximum constant-

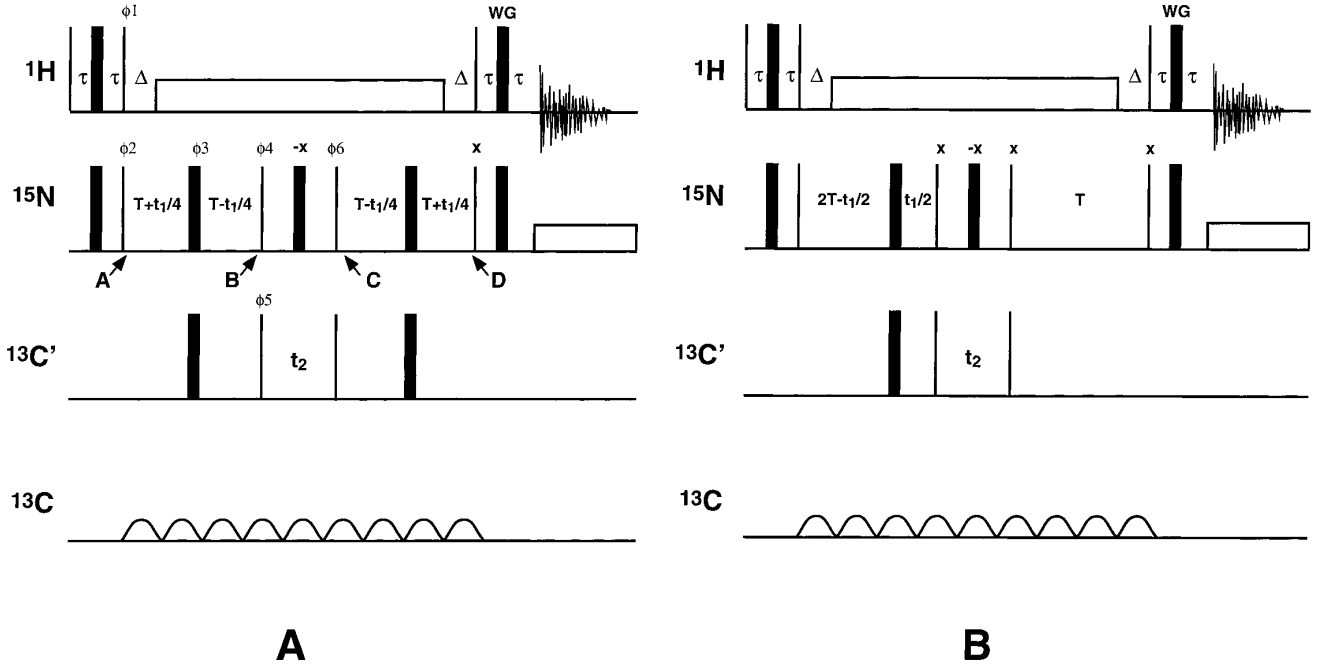

A **B**

FIG. 1. (A) Pulse sequence for the 2CT-HNCO experiment in which both ^{15}N–^{13}C′ polarization transfer periods (length $2T$ = 25 ms) are evolved. Fixed delays are τ = 2.25 ms and Δ = 5.4 ms; WG denotes a WATERGATE solvent suppression sequence (*18*); SEDUCE-1 (*19*) is used for selective carbon decoupling. The following phase cycle was used: $\phi1 = (y, -y)$, $\phi2 = x$, $\phi3 = (x, x, x, x, y, y, y, y)$, $\phi4 = x$, $\phi5 = (x, x, -x, -x)$, $\phi6 = x$, rec = $(x, -x, -x, x, -x, x, x, -x)$. Phase sensitive indirect evolution is accomplished by the incrementation of $\phi2$ and $\phi5$ according to the States–TPPI protocol (*20*). A truncated (two-step) phase cycle can be used by the proper placement of gradients to correct for pulse imperfections and to achieve coherence selection (*11*). Points A–D are discussed in the text. (B) The ''full-sweep'' implementation of the 2CT-HNCO experiment.

1090-7807/98 $25.00

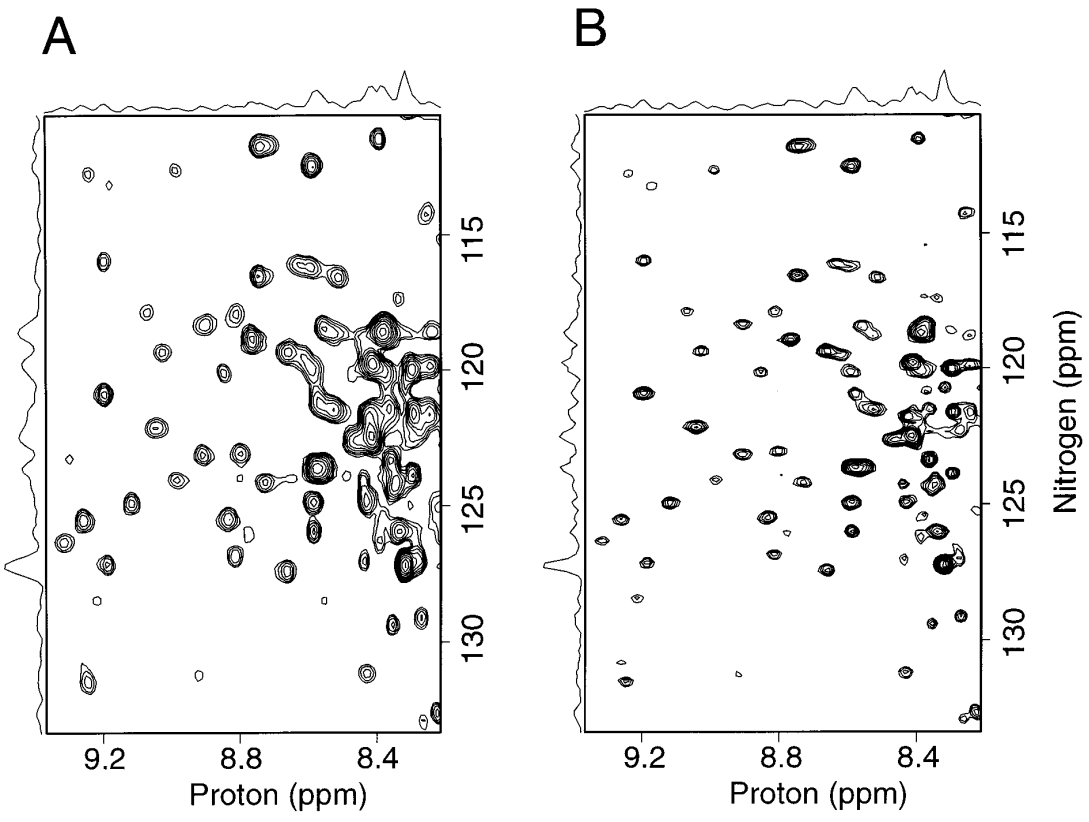

FIG. 2. A comparison of the $^{1}HN/^{15}N$ 2D plane from (A) the CT-HNCO of Ref. (*3*) and (B) 2CT-HNCO from Fig. 1A. For the CT-HNCO data set, 50 complex points were acquired in the ^{15}N (t_1) dimension by incrementing (or decrementing) each $t_1/2$ by 250 μs; 16 scans per FID were used. The 2CT-HNCO data set was recorded with 100 complex points in t_1 with each $t_1/4$ increment/decrement of 125 μs; 8 scans per FID were used.

time ^{15}N evolution period, the indirect *X* spin is evolved as multiple-quantum coherence. Polarization transfer involving a passive spin (for example, CO in the HN(CO)CA experiment) is also accomplished in an HMQC manner. Vuister and Bax used a double constant-time (2CT) evolution scheme in the 3D HNHA double resonance experiment (*8*) which also evolves both indirect dimensions as MQ coherence. Van Doren and Zuiderweg (*9*) have presented an experiment that simultaneously evolves multiple- and single-quantum coherence and have applied it to the evolution of $C_\alpha - H_\alpha$ coherence. Our approach (*10*) is to evolve the *X* spin as both multiple- and single-quantum coherence to allow for the double constant-time ^{15}N evolution in all HN*X* experiments where N-to-*X* transfer may include a transfer to a passive spin. Our work extends the 2CT evolution scheme to triple-resonance 3D experiments and introduces 4CT evolution (two 2CT periods) in a 4D heteronuclear correlation experiment. The modifications needed to accomplish 2CT evolution in triple-resonance experiments are straight forward, are completely general, and consequently, will yield increased resolution for all out-and-back experiments.

The 2CT-HNCO experiment is sketched in Fig. 1A. A $\pi/2$ pulse at point A initiates $^{15}N_y$ coherence that is transferred to $^{13}C'_z$ polarization during 2*T*. Nitrogen chemical shift evolution occurs in a constant-time fashion, resulting in a mixture of $^{15}N_y$ and $^{15}N_x$ components at the end of 2T. A pair of $^{13}C/^{15}N$ 90° pulses at point B establishes $^{13}C'$ coherence that is evolved during t_2: ^{15}N magnetization is stored as a mixture of longitudinal (N_z) and transverse ($N_{x,y}$) components. At this point our sequence is identical to that in Ref. (*3*). Carbon evolution is terminated and nitrogen coherence is reestablished at point C by another pair of $^{13}C/^{15}N$ $\pi/2$ pulses. To date, all reported HN*X* experiments select either single-quantum or multiple-quantum heteronuclear coherence at point C (terms $\sim N_x C_{x,y}$ or $\sim N_{x,y} C_{x,y}$, respectively) that is ultimately converted to detectable proton magnetization. In our approach, both single-quantum and multiple-quantum heteronuclear coherence that is present between points B and C is transferred to transverse ^{15}N magnetization at point C, and can be further evolved during the 2*T* back transfer delay between points C and D. Sensitivity enhancement (*5*) may be used to transfer both N_x and N_y components at point D to proton magnetization. Sensitivity enhancement is not always beneficial, however, due to relaxation losses that occur during the $1/2J_{HN}$ extension of the pulse that is required to simultaneously detect both components. Relative

to the HNCO pulse sequence in Ref. (*3*), a simple modification of the phase of one or both of the ^{15}N $\pi/2$ pulses (shown at points B and C in Fig. 1) results in ^{15}N evolution as single-quantum coherence ($\sim N_{x,y}C_z$) between points A and B and also between points C and D while $^{13}C'$ coherence is evolved as a mixture of heteronuclear single- and multiple-quantum coherence $(N_z + N_{x,y})C_{x,y}$ between points B and C in Fig. 1. The effect of evolving mixed single- and multiple-quantum coherence has been characterized (*9*) in similar applications. In the 2CT-HNCO experiment these effects are expected to be small because of the relatively long relaxation times for both types of coherence. Since the $^{13}C'-{}^{13}C_\alpha$ scalar coupling is removed, $^{13}C'$ evolution times can be lengthened which might create artifacts from differential relaxation. These artifacts would appear in the carbon dimension as quadrature peaks. They can be eliminated using pulsed field gradients, but represent a potential loss in sensitivity. We do not observe these artifacts with either ubiquitin (76 residues) or MMP-1 (170 residues) but they might arise in higher signal-to-noise data sets or in larger proteins where the ^{15}N T_2 is shorter. In a 2CT-HNCA experiment (for which the sequence in 1A can be used by simply interchanging the $^{13}C'$ and $^{13}C_\alpha$ pulses) $^{13}C_\alpha$ evolution is typically limited to $\sim$7 ms so as not to resolve $^{13}C_\beta-{}^{13}C_\alpha$ scalar coupling and $T_2(^{15}N)$ is typically long compared with $T_2(^{13}C_\alpha)$. A significant difference in relaxation could arise when the $^{13}C_\alpha$ evolution is lengthened, for example, when constant-time $^{13}C_\alpha$ evolution is used to filter $^1H-{}^{13}C_\alpha$ from $^2H-{}^{13}C_\alpha$ in fractionally deuterated proteins (*11*) or when $^{13}C_\beta$ decoupling is used to extend $^{13}C_\alpha$ evolution (*12, 13*).

Figure 1B shows another implementation of the pulse sequence in the ''full-sweep'' ^{15}N evolution, whereas Fig. 1A is a ''double constant-time'' implementation. In both pulse schemes, longitudinal and transverse components of ^{15}N magnetization are restored to purely transverse (rotating) components that are evolved during the back polarization transfer period. In both experiments, a factor of 2 is gained in nitrogen resolution without suffering any loss in sensitivity.

Data from a 2CT-HNCO experiment is compared to the CT-HNCO (3) in Fig. 2. In Fig. 2A, 50 complex points (corresponding to 25 ms of t_1 evolution) were acquired in the ^{15}N dimension of the CT-HNCO, while in Fig. 2B, 100 complex points were acquired (corresponding to 50 ms of t_1 evolution) with the 2CT scheme in Fig. 1A. The number of scans was 16 and 8 for 2A and 2B, respectively, to enable comparison of the experiments of an equal total duration. After linear prediction (not used in any of our spectra) and zero filling, the digital resolution in the ^{15}N dimension is 5.0 Hz. The protein used to collect these spectra is the 19-kDa catalytic domain of the metalloproteinase MMP-1 (*14*). Data on a 0.6 mM, $^{13}C/{}^{13}N$-labeled sample were collected on a Bruker DMX 600 spectrometer at a temperature of 30° and a pH of 6.5. Note that the resolution gain is shown by separation of peaks in the 2D contours and the 1D vertical projection, while the horizontal projections (the sum of ^1HN vectors) are identical.

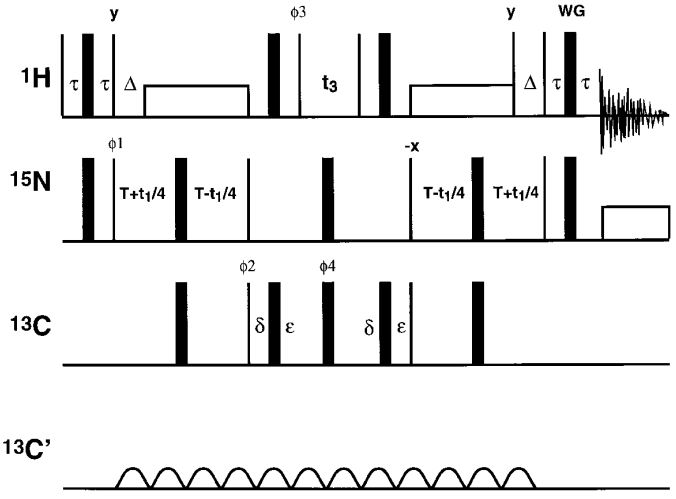

FIG. 3. Pulse sequence for the 4CT-HNCAHA experiment where both ^{15}N and ^{13}C dimensions use 2CT evolution. The delay $2T$ is optimized for $^{15}N-{}^{13}C_\alpha$ polarization transfer; ^{15}N coherence is evolved during both $2T$ transfer delays using constant-time incrementation. Fixed delays are τ = 2.25 ms and Δ = 5.4 ms; WG denotes a WATERGATE solvent suppression sequence (*18*); SEDUCE-1 (*19*) was used for selective carbon decoupling. The variable delays $\delta = 1.5\ m + t_2/4$ and $\epsilon = 1.5\ m - t_2/4$ allow for $^{13}C_\alpha-{}^1H_\alpha$ polarization transfer and also encode the $^{13}C_\alpha$ chemical shift using the 2CT scheme. The following phase cycle was used: $\phi1 = (x, x, -x, -x)$, $\phi2 = x$, $\phi3 = (x, -x)$, $\phi4 = (x, x, x, x, y, y, y, y)$, rec = $(x, -x, -x, x, -x, x, x, -x)$. Phase sensitive indirect evolution is accomplished by the incrementation of $\phi1$, $\phi2$, and $\phi3$ according to the States–TPPI protocol (*20*).

Figure 3 is an implementation of 2CT evolution to both the ^{15}N and ^{13}C evolution periods of the HNCAHA experiment (*15, 16*). Here we use a pulse timing diagram that most resembles that outlined in Ref. (*15*) but we eliminate the semi-constant-time $^{13}C_\alpha$ evolution and instead use a 2CT $^{13}C_\alpha$ evolution scheme that is achieved by incrementing the delays δ and ε as shown. 2CT ^{15}N evolution is achieved exactly as in our example of the HN*X* experiment. Other modifications include the evolution of $^1H_\alpha-{}^{13}C_\alpha$ as multiple-quantum coherence (*16*) and the inclusion of a central ^{15}N refocusing pulse during $^1H_\alpha$ evolution. The ^{15}N π pulse is not used for *J* refocusing but for ^{15}N chemical shift refocusing during the transfer from C_α and H_α and refocusing during the delay for $^1H_\alpha$ evolution. A comparison of the 2D $^1HN/{}^{15}N$ plane from the experiment in Fig. 3 to that in Ref. (*15*) is given in Fig. 4. While it might be impractical to collect a 4D with 100 complex points in one dimension, (1) the ^{15}N spectral width may need to be reduced for some samples, and (2) not all of the total $4T$ transfer period needs to be evolved. Furthermore, the 4CT-HNCAHA serves as a template for the use of 2CT evolution in experiments involving transfer through a passive spin, such as the HN(CO)CA (*2*), HN(CA)CB, and HN(COCA)CB (*11*) experiments.

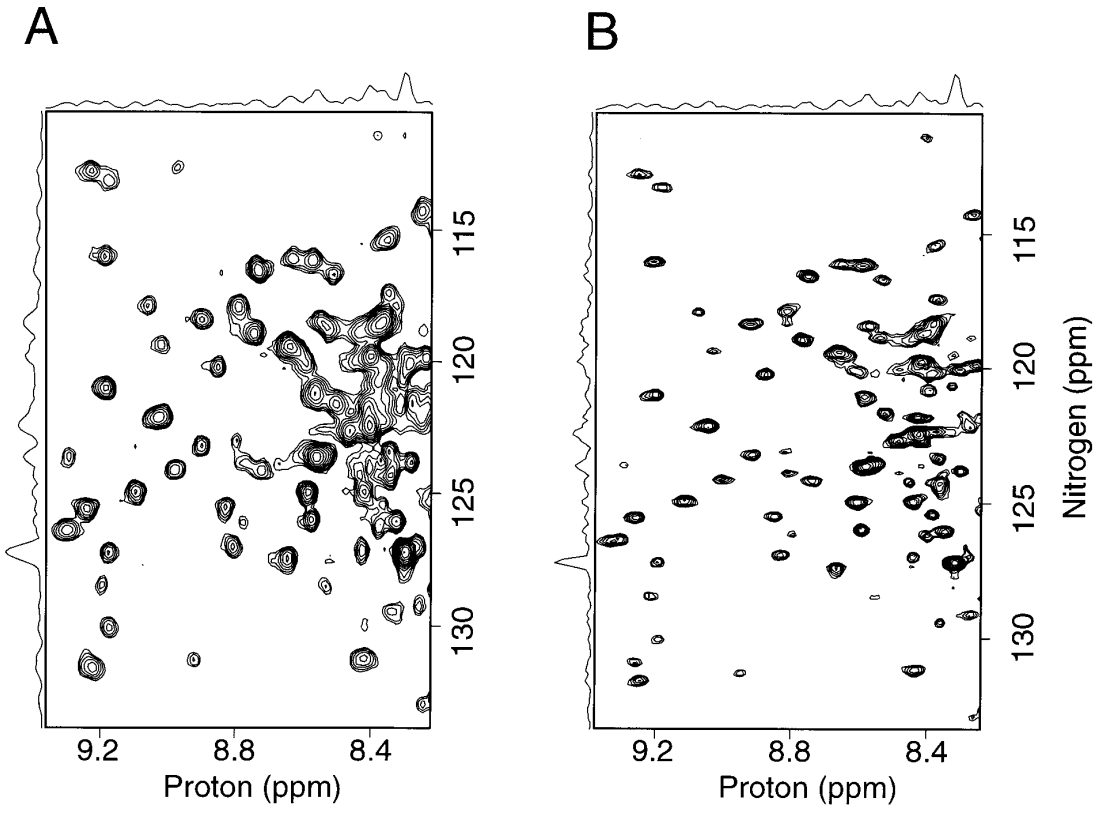

FIG. 4. A comparison of the $^{1}HN/^{15}N$ 2D plane from (A) the HNCAHA of Ref. (*15*) and (B) 4CT-HNCAHA from Fig. 3. For the HNCAHA data set, 50 complex points were acquired in the ^{15}N (t_1) dimension with 64 scans per FID. The 4CT-HNCAHA data set was recorded with 100 complex points and 32 scans per FID. The $t_1/2$ and $t_1/4$ increments for (A) and (B) were, respectively, 250 and 125 μs. The data that are shown correspond to the same spectral region shown in Fig. 2. Slight differences between the peaks in these spectra and those in Fig. 2 are due to glycine residues which do not have HNCAHA correlations in this implementation. Of course, a full 3D or 4D would require the use of fewer scans per point, fewer ^{15}N points, and a maximum of 20–24 points (6.0 ms) to be collected in the $^{13}C_{\alpha}$ dimension.

Constant-time evolution during polarization transfer allows for evolution of indirect spins without increasing the length of the pulse sequence. The amount of time that can be evolved is limited to the length of the constant-time polarization transfer delay which is set in accordance with the heteronuclear scalar coupling. By simple modifications of ''out-and-back'' pulse sequences, we are able to double the maximum possible evolution without sacrificing any sensitivity. Other methods of resolution enhancement have made use of the constant-time polarization transfer delays (*3, 4, 7–10, 15, 16*). Recently Bauer and Kessler (*17*) have presented a scheme based on the HMQC evolution reported by Sørensen (*7*), only they report a substantial loss in sensitivity in order to achieve improved resolution. The alterations that we describe are straightforward, require no additional pulses, and suffer no loss in sensitivity. Additionally, 2CT and 4CT evolution will work on any existing ''out-and-back'' sequence, regardless of the type of coherence that is evolved. The two examples presented here should provide a template for the inclusion of 2CT evolution into any out-and-back 3D or 4D heteronuclear correlation experiment. We expect that the increased resolution of the 2CT and 4CT evolution presented here will be useful in the study of larger, partially folded proteins, and in study of highly helical proteins where ^{1}HN, ^{15}N, and ^{13}C dimensions are poorly dispersed.

ACKNOWLEDGMENTS

The author thanks Stanley Opella for his support of this work and Ole Sørensen for his comments and suggestions. This work was supported by Grant R823576 from the Environmental Protection Agency.

REFERENCES

1. L. E. Kay, M. Ikura, R. Tschudin, and A. Bax, Three-dimensional triple-resonance NMR spectroscopy of isotopically enriched proteins, *J. Magn. Reson.* **89,** 496–514 (1990).
2. A. Bax and M. Ikura, An efficient 3D NMR technique for correlating the proton and ^{15}N backbone amide resonances with the α-carbon of the preceding residue in uniformly $^{15}N/^{13}C$ enriched proteins, *J. Biomolec. NMR* **1,** 99–104 (1991).
3. S. Grzesiek and A. Bax, Improved 3D triple-resonance NMR techniques applied to a 31 kDa protein, *J. Magn. Reson.* **96,** 432–440 (1992).

4. A. G. Palmer, W. J. Fairbrother, J. Cavanagh, P. E. Wright, and M. Rance, Increased resolution in three dimensional constant-time triple resonance NMR spectroscopy of proteins, *J. Biomolec. NMR* **2,** 103–108 (1992).
5. J. Cavanagh, A. G. Palmer, P. E. Wright, and M. Rance, Sensitivity improvement in proton detected two-dimensional heteronuclear relay spectroscopy, *J. Magn. Reson.* **91,** 429–436 (1991).
6. S. Grzesiek and A. Bax, The importance of not saturating H_2O in protein NMR. Applications to the sensitivity enhancement of NOE measurements. *J. Am. Chem. Soc.* **115,** 12,593–12,594 (1993).
7. J. C. Madsen and O. W. Sørensen, Multidimensional NMR experiments with improved resolution, *J. Magn. Reson.* **100,** 431–436 (1992).
8. G. W. Vuister and A. Bax, Quantitative J correlation: A new approach for measuring homonuclear three-bond $J(H^NH^\alpha)$ coupling constants in ^{15}N-enriched proteins, *J. Am. Chem. Soc.* **115,** 7772–7777 (1993).
9. S. R. Van Doren and E. R. P. Zuiderweg, Improvements in HSMQC-type double- and triple-resonance NMR experiments by using full-sweep (semi-) constant-time shift labeling, *J. Magn. Reson. B* **104,** 193–198 (1994).
10. M. A. McCoy, 36th Experimental NMR Conference, Boston, MA, 1995.
11. T. Yamazaki, W. Lee, C. H. Arrowsmith, D. H. Muhandiram, and L. E. Kay, A suite of triple resonance NMR experiments for the backbone assignment of ^{15}N, ^{13}C, and ^{2}H labeled proteins with high sensitivity, *J. Am. Chem. Soc.* **116,** 11,655–11,666 (1994).
12. M. A. McCoy, Selective refocusing of C_β scalar coupling during indirect evolution of heteronuclear single-quantum carbon coherences, *J. Magn. Reson. B* **107,** 270–273 (1995).
13. Ē. Kupče and G. Wagner, Multisite band-selective decoupling in proteins, *J. Magn. Reson. B* **110,** 309–312 (1996).
14. M. A. McCoy, M. J. Dellwo, D. M. Schneider, T. M. Banks, J. Falvo, K. J. Vavra, A. M. Mathiowetz, M. W. Qoronfleh, R. Ciccarelli, E. R. Cook, T. A. Pulvino, R. C. Wahl, and H. Wang, Assignments and structure determination of the catalytic domain of human fibroblast collagenase using 3D/4D double and triple resonance NMR spectroscopy, *J. Biolmolec. NMR* **9,** 11–27 (1997).
15. E. T. Olejniczak, R. X. Xu, A. M. Petros, and S. W. Fesik, Optimized constant-time 4D HNCAHA and HN(CO)CAHA experiments. Applications to the backbone assignments of the FKBP/ascomycin complex, *J. Magn. Reson.* **100,** 444–450 (1992).
16. L. E. Kay, M. Wittekind, M. A. McCoy, M. S. Friedrichs, and L. Mueller, 4D NMR triple-resonance experiments for assignments of protein backbone nuclei using time shared constant-time evolution periods, *J. Magn. Reson.* **98,** 443–450 (1992).
17. M. Baur and H. Kessler, An easy way for resolution enhancement in out-and-back triple resonance experiments applied to the HCACO sequence, *J. Magn. Reson.* **126,** 270–273 (1997).
18. M. Piotto, V. Saudek, and V. Sklenář, Gradient-tailored excitation for single-quantum NMR spectroscopy of aqueous solutions, *J. Biomolec. NMR* **2,** 661–665 (1992).
19. M. A. McCoy and L. Mueller, Selective shaped pulse decoupling in NMR: Homonuclear ^{13}C carbonyl decoupling, *J. Am. Chem. Soc.* **114,** 2108–2112 (1992).
20. D. Marion, M. Ikura, R. Tschudin, and A. Bax, Rapid recording of 2D NMR spectra without phase cycling. Applications to the study of hydrogen exchange in proteins, *J. Magn. Reson.* **85,** 393–399 (1989).